Article

Phenolic 3° Phosphine Oxides as a Class of Metal-Free Catalysts for the Activation of C–O Bonds in Aliphatic Alcohols: Direct Synthesis of Catalyst Candidates, and Kinetic Studies

Matthew A. Martin, Sadie L. Brown, Danielle R. Beres, Wrebekah M. Frederic, Ashley M. Banks and Aaron J. Bloomfield *

Department of Chemistry and Biochemistry, Duquesne University, 600 Forbes Ave., Pittsburgh, PA 15282, USA; martinm12@duq.edu (M.A.M.); browns20@duq.edu (S.L.B.); beresd@duq.edu (D.R.B.); fredericw@duq.edu (W.M.F.); banksa2@duq.edu (A.M.B.)
* Correspondence: bloomfielda@duq.edu or ajbloomfield256@gmail.com

Abstract: It was recently reported that a (2-hydroxybenzyl)phosphine oxide (2-HOBPO) can serve as a phosphorus-centered catalyst for the stereo-invertive coupling of aliphatic alcohols and acidic pronucleophiles (akin to a Mitsunobu reaction, but without additional reagents). Herein, we report an improved synthesis, which provides direct access to systematically varied 2-HOBPOs in a single step from commercially available precursors (salicylaldehydes and secondary phosphines). The efficiency and generality of the synthetic method enabled limited structure–activity relationship (SAR) studies, from which it was determined that substituents on both the phenolic and phosphine oxide portions can exert significant influence on the turnover frequency (TOF) of each catalyst. Importantly, for all catalytically active 2-HOBPOs examined, the molecularity of catalyst in the rate law of the alcohol coupling was determined to be <1. Thus, for high catalyst loadings, differences in catalytic activity between 2-HOBPOs appear to be dominated by differences in catalytic auto-inhibition, while for low catalyst loadings, differences are attributed to inherent differences in the energetic span of the catalytic cycle, ignoring off-cycle species, in good agreement with density functional theory (DFT) modeling at the ωB97X-D/6-311G(d,p) level.

Keywords: phosphine oxide; alcohol activation; Mitsunobu reaction; organocatalysis

1. Introduction

The Mitsunobu reaction (Figure 1a) is of particular importance in the fields of synthetic organic chemistry and medicinal chemistry and is the topic of several reviews (from the perspective of synthetic organic chemists) [1–3]. This protocol allows aliphatic alcohols to serve as electrophiles for S_N2 substitution, and in cases in which the O-bound carbon atom of the alcohol is a stereocenter, the reaction is highly selective for inverting the configuration of the stereocenter. Alcohols are otherwise fairly unreactive in general, and specifically extremely poor as electrophiles for S_N2 substitution reactions, but due to their ubiquity and generally non-hazardous nature, alcohols are considered to be desirable raw materials and synthetic intermediates. Accordingly, the development of new methods capable of selectively transforming alcohols into other functional groups has been identified as an important objective on the path to a greener chemical industry.

Traditional Mitsunobu conditions overcome the inherent lack of reactivity of alcohols by deploying both a reducing agent such as a tertiary phosphine (O-atom sink) and an oxidizing agent such as diethyl azodicarboxylate (H-atom sink). In addition, although the Mitsunobu protocol is a powerful and selective synthetic tool, this reaction suffers from very poor atom economy (often <35%), and the byproducts can be difficult to remove from the crude product mixture. Most advances in this methodology over the past 50 years have

been centered on the development of improved reagents [2–5], conferring greater selectivity [4] or easier separation of byproducts [5], neither of which addresses the inherently low atom economy.
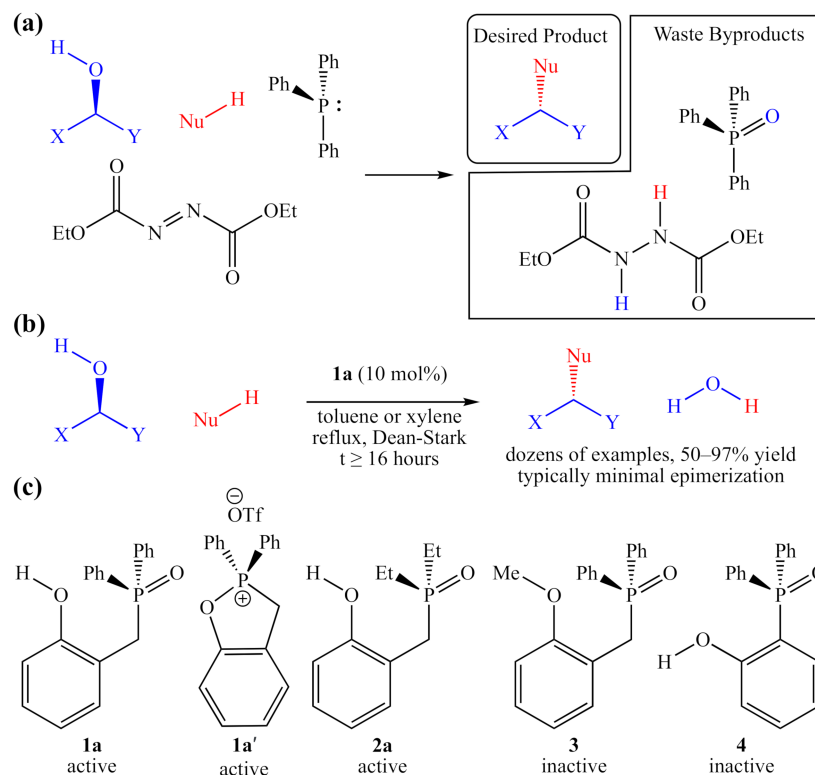

Figure 1. (**a**) A balanced generic traditional Mitsunobu reaction, using stoichiometric quantities of triphenylphosphine and diethyl diazodicarboxylate; (**b**) catalytic "Redox-Neutral" Mitsunobu reaction examined by Denton and co-workers; (**c**) active and inactive catalyst candidates examined by Denton and co-workers, and **2a**, which is also active.

There have been some reports of systems that employ catalytic amounts of phosphine [6] or other redox mediators [7], but they still require stoichiometric amounts of both a terminal reductant (such as silane) and a terminal oxidant (such as O_2). The first system to require no reagents other than the two coupling partners was reported in 2019, by Denton and co-workers [1]. This purely catalytic "redox-neutral Mitsunobu reaction" was promoted using a substoichiometric amount of a bifunctional phenolic tertiary phosphine oxide (TPO), **1a** as an organocatalyst (Figure 1b). Recently, a polymer-bound version of this catalyst was shown to be similarly active and easily recovered [8].

In addition to demonstrating the wide scope of alcoholic substrates that this system can couple with a modest range of acidic pronucleophiles (Nu–H), the authors reported a very limited structure–activity relationship (SAR) study, identifying two catalytically active compounds (**1a** and **1a′**), which appear to enter into the same catalytic cycle (manifold), as well as two analogs, which were reported to be completely inactive (Figure 1c). While playing a crucial role in probing the mechanism of this catalyst class, these studies provide no information about trends in activity or selectivity. Instead of removing functional groups from the catalyst, modifications can be made to existing functionality to examine how more subtle changes influence activity. For example, it is shown in this manuscript that the diethylphosphinoyl analog **2a** is also catalytically active.

Based on the relative activities of **1a**, **1a′**, **3**, and **4**, as well as ^{18}O isotope-labeling studies, Denton and co-workers proposed a three-step catalytic cycle (Figure 2), in which there is a dehydrative cyclization (step A), generating intermediate **1a′**, which then reacts with the alcohol (step B) to provide the activated alcohol, **1a″**, which then undergoes a

nucleophilic attack (step C) affording the product and regenerating **1a**. This simple and reasonable cycle is supported by all of their experimental evidence. However, a recent computational examination [9] of this reaction reported a more complex catalytic cycle with well-defined elementary steps and explicit transition states, with energies determined by DFT methods (using the ωB97X-D functional [10] with the 6-311G(d,p) basis set). The report did not indicate any significant deactivation reactions or off-cycle states; however, it is unclear whether they were sought after. If there are no off-cycle resting states, the turnover frequency of the catalyst should be almost entirely determined by the energetic span of the catalytic cycle (the difference in energy between the lowest minimum and highest transition state along the catalytic cycle) [11]. The lowest ground state and highest transition state identified in this study (Figure 3) correspond to an H-bonded complex of **1a** and the pronucleophile, and the nucleophilic attack on the activated alcohol. Destabilization of the lowest energy state and stabilization of the highest transition relative to each other should lead to more efficient catalysts.
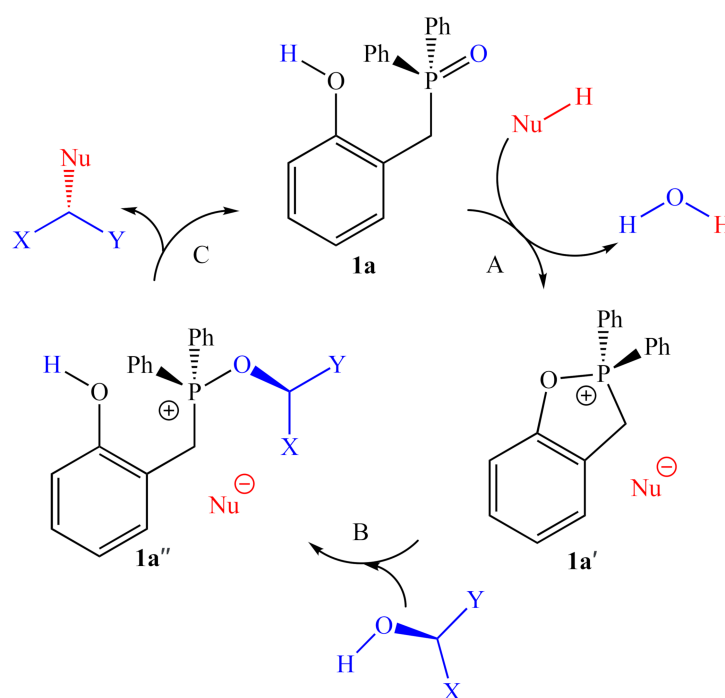
Figure 2. The catalytic cycle proposed by Denton and co-workers.
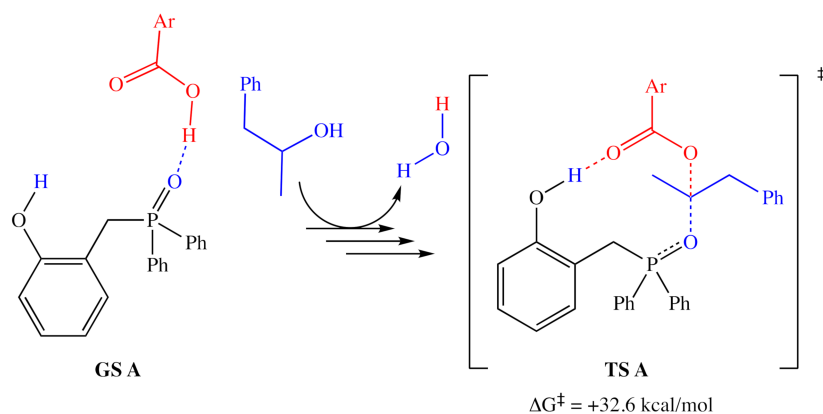

Figure 3. The resting state (**left**) and highest energy transition state (**right**) proposed by Houk and co-workers. Calculated energy accounts for both consumed alcohol and produced water. Ar = 2,4-dinitrophenyl.

The scope of alcohols activated by both **1a** and polymer-supported **1a** under the reported conditions [1,8] is quite large, including 1° and 2° alcohols, and tolerating functional groups such as primary alkyl bromides [12] and azides, [13] which would react readily with the tertiary phosphines required for classical Mitsunobu reactions, but which are inert towards TPOs. In general, the reactions proceeded with high yields and little to no erosion of enantioenrichment, with inversion of the configuration of the center of substitution, as typically observed for Mitsunobu reactions.

However, this method suffers from some significant limitations as well. As reported, the reaction is very slow, with apparent turnover frequencies in the order of one turnover per day, even at the very high temperatures of refluxing xylenes (ca. 140 °C). Because of the extremely low TOF, Denton and co-workers reported using high catalyst loadings (10–25 mol%) and long reaction times (20–96 h) at 110–160 °C. Due to the high catalyst loadings, only low turnover numbers (up to 10) were found.

Perhaps more importantly, in contrast to the PPh$_3$/DEAD protocols, which are effective for coupling pronucleophiles with pK$_a$ values between 0 and 11 [2,3], Denton and co-workers reported a complete lack of activity for pronucleophiles with pK$_a$ values above 3.5 (all pK$_a$ values discussed in this manuscript refer to aqueous values, unless otherwise specified), and Pericàs and co-workers also only report reactions for highly acidic pronucleophiles. The preferred pronucleophile in both studies was 2,4-dinitrobenzoic acid (2,4-DNBA), with a pK$_a$ of 1.4.

Based on conversion/yields, catalyst loadings, reaction times, and temperatures reported in the SI accompanying their report [1], the apparent energetic span [11] of **1a**-facilitated esterification reactions of 2-octanol and variously substituted benzoic acid pronucleophiles can be calculated. Although only five data points are available, the energetic spans appear to be very strongly linearly correlated to the pK$_a$ of the pronucleophile (Figure 4). This suggests that the dissociation of the pronucleophile is either involved in the rate-determining step (as proposed by Denton [1]), or as rapid equilibrium preceding the rate-determining step (as proposed by Houk [9]). In either case, it would be reasonable to hypothesize that an increase in the basicity of the TPO could improve the scope of pronucleophiles that can be activated. This can be accomplished by adding electron-donating groups to the phosphorus-bound phenyl rings, or by removing the aromatic rings entirely and replacing them with aliphatic substituents. It has been shown experimentally that, in nitromethane, Et$_3$POH$^+$ has a pK$_a$ ca. 1.5 units higher than EtPh$_2$POH$^+$. Ref. [14] If the upper pK$_a$ limit of pronucleophiles could be increased by a similar margin (up to a pK$_a$ of 5), this could allow for the activation of most carboxylic acids.
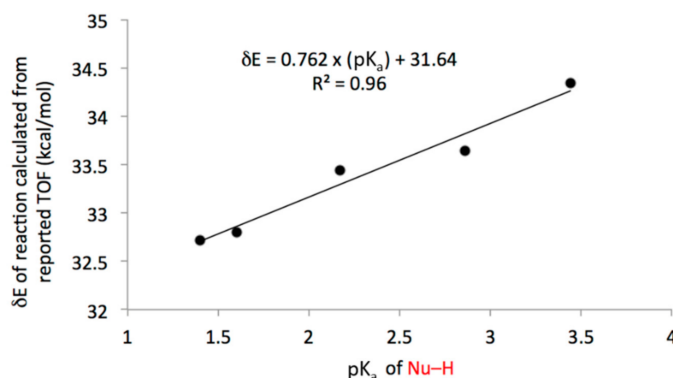
Figure 4. Apparent energetic span of the esterification of 2-octanol facilitated by **1a** as a function of the pK$_a$ of the pronucleophile (from left to right: 2,4-dinitrobenzoic acid, pentafluorobenzoic acid, 2-nitrobenzoic acid, 2-iodobenzoic acid, 4-nitrobenzoic acid).

Unfortunately, the reported [1] three-step synthesis of **1a** (Figure 5a) is not conducive to preparing large numbers of analogs and is likely to be severely limited in terms of the scope of potential products accessible through this route because of the harsh reagents

involved (PBr$_3$, NaH, and BBr$_3$). For instance, the final step of the synthesis uses excess BBr$_3$ to demethylate an aryl methyl ether to reveal the final 2-HOBPO catalyst. This deprotection strategy precludes the preparation of analogs containing strongly electron-donating methoxy substituents as well as analogs containing electron-withdrawing ester substituents. Similarly, the use of PBr$_3$ and NaH complicates the synthesis of analogs containing nucleophilic or protic functionality.
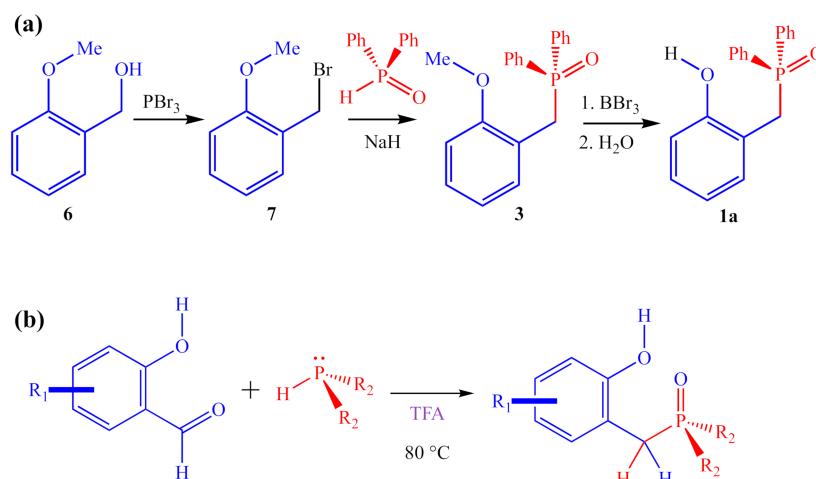
Figure 5. (**a**) Multi-step synthesis of **1a** reported by Denton and co-workers; (**b**) ARC synthesis to access diverse array of 2-HOBPOs in a single step.

Alternative synthetic approaches to generating 2-HOBPOs include the direct addition of secondary phosphine oxides to *ortho*-quinone methides (either premade or generated in situ) [15], or by addition of diethyl phosphite, followed by treatment with Grignard reagents, which has previously been used to prepare **2a** [16]. However, the most generalizable method appears to be by an addition–rearrangement coupling (ARC) reaction (Figure 5b) [17–19].

In this manuscript, we apply the DFT-based model system reported by Houk and co-workers to eight systematically varied 2-HOBPO analogs, and report the direct, single-step synthesis of 2-HOBPO catalyst candidates bearing a diphenylphosphinoyl (**1x**) or diethylphosphinoyl (**2x**) group from commercially available 2° phosphine and commercially available salicylaldehydes, using an ARC reaction. These catalyst candidates were compared on the basis of their activity for the coupling of 2-octanol and 2,4-DNBA. Additionally, initial rates kinetics studies were performed with varying concentrations of each catalyst candidate, as well as varying concentrations of 2-octanol and 2,4-DNBA (only with **1a**). Finally, the computational models of possible catalytic cycles for the different catalyst candidates were compared with experimental findings.

2. Results

2.1. DFT Calculations

DFT modeling was performed using nearly the same methods as reported by Houk and co-workers [9]: Gas-phase calculations with polarizable continuum model (PCM) to approximate the dielectric constant of xylenes and the ωB97X-D functional with the 6-311G(d,p) basis set. The only difference was that the present study used a temperature of 413.15 K (140 °C), instead of 298.15 K (25 °C) for the energy corrections. This change contributes to relatively subtle differences in the thermal corrections to enthalpy, based on the contribution of thermally populated vibrational modes, as well as significant changes in how the entropic terms are scaled when performing the Gibbs free energy correction—this is most important when considering reactions that increase or decrease the number of degrees of freedom (such as dissociation, cyclization, or the opposite reactions).

2.1.1. Alternative Resting State and Transition States

Before structural analogs of **1a** were examined computationally, potential alternative ground states and transition states were identified and included for comparison. Multiple stable alternative ground states for the **1a**/2,4-DNBA/2-phenylpropanol system were identified (Table 1, rows 1–5), including several that were found to be more stable than the lowest ground state identified by Houk and co-workers (**GS A**) [9]. The most stable of these (**GS B**) was between 5 and 10 kcal/mol more stable than **GS A**, depending on the method used, and whether enthalpies or free energies were compared. Computed relative energies for all structures depended somewhat on the methods employed (Table 2). Structures were optimized and energies calculated using B3LYP/6-31G, which is known to overestimate the stability of hydrogen bonds [20], as well as the ωB97X-D/6-311G(d,p), which was used for all other calculations discussed in this manuscript.

However, both methods predicted the same ordering of energies, which span significantly less than the >30 kcal/mol energetic span of the catalytic cycle. Interestingly, **GS B** contains an intramolecular H-bond between the phenol and phosphine oxide, as well as an intermolecular H-bond between the pronucleophile and the phosphine oxide (Figure 6), which suggests that the acidity of the phenol may be important for both the global GS and global TS.

In addition to the highest energy transition state of the catalytic cycle identified by Houk and co-workers (**TS A**, sixth row of Table 2), one alternative structure for the highest energy transition state was identified (**TS B**, final row of Table 2), in which the phenolic hydrogen of the catalyst forms a hydrogen bond with the oxygen of the activated alcohol, rather than with the incoming carboxylate nucleophile.

It was initially hypothesized that, by changing the hydrogen bond acceptor from the incoming nucleophile to the outgoing nucleofuge, the structure would correspond to a more electrophilic activated alcohol and a more nucleophilic carboxylate, and therefore represent a lower activation barrier. However, it appears that the energy penalty for simultaneously generating both reactive partners more than outweighs their enhanced reactivity. There may be other energetically relevant transition states in this manifold, especially those including additional equivalents of catalyst or pronucleophile explicitly interacting with the reactive partners, but we did not look for those.
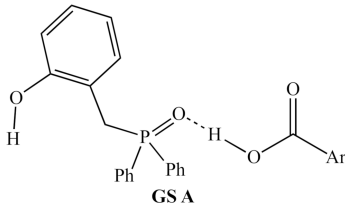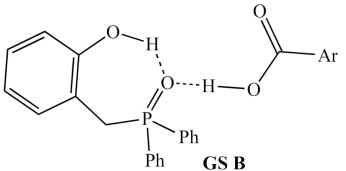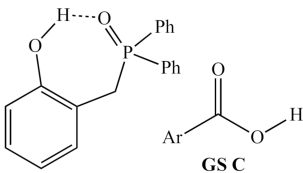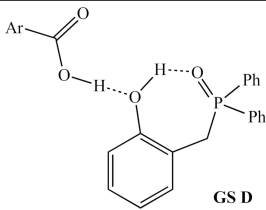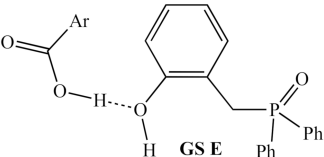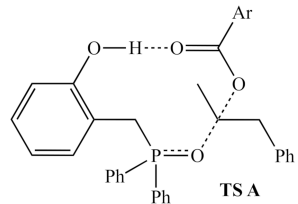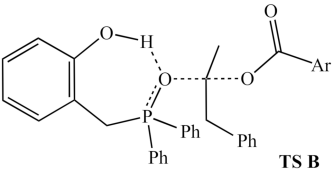
Note that to compare the energies of **TS A** or **TS B** with those of **GS A** or **GS B**, the energies of produced water and consumed 1-phenylpropan-2-ol were also modeled as free molecules in the gas phase, using the same functional, basis set, temperature, and implicit solvent.

2.1.2. Structural Analogs

Using the computed intermediates and transition states of the **1a**/2,4-DNBA/2-phenylpropanol system as starting templates, structural modifications were made, and then each structure was re-optimized. Results are summarized in the schemes below for modified 2-HOBPOs in which the substituent *para* to the phenol is a hydrogen, methyl, methoxy, or nitro group, and the substituents on phosphorus are phenyl groups (**1x**) or methyl groups (**2x***). The *P*-methyl derivatives (**2x***) were used for computational models instead of the ethyl derivatives (**2x**) to reduce the computational expense by decreasing the number of orbitals and the number of degrees of freedom without significantly changing either the steric or electronic properties.

For all 2-HOBPOs examined, an alternative transition state (**TS B**) was found to be significantly higher in free energy (>5.5 kcal/mol) than the transition state identified by Houk (**TS A**) and could be safely ignored. However, it also does appear that the energy of this transition state is much more sensitive to the nature of the catalyst structure, with electronic energies differing by up to 3.7 kcal/mol across the eight analogs, compared to a span of only 2.9 kcal/mol for analogs of **TS A**, and therefore could potentially be relevant in the catalytic cycles of other, more different 2-HOBPO catalysts.
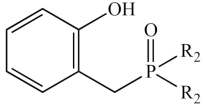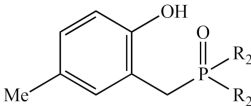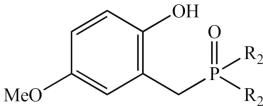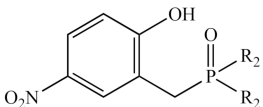
Table 1. Possible turnover-limiting ground state and transition state structures for the **1a**-mediated reaction of 2,4-DNBA and 1-phenylpropan-2-ol.

Structural Representation [1]	Method	ΔH [2]	$\Delta G^{413.15}$
GS A	B3LYP/ 6-31G	+8.4 kcal/mol	+6.9 kcal/mol
	ωB97X-D/ 6-311G(d,p)	+5.2 kcal/mol	+6.0 kcal/mol
GS B	B3LYP/ 6-31G	0 kcal/mol	0 kcal/mol
	ωB97X-D/ 6-311G(d,p)	0 kcal/mol	0 kcal/mol
GS C	B3LYP/ 6-31G	+22.2 kcal/mol	+5.1 kcal/mol
	ωB97X-D/ 6-311G(d,p)	+20.4 kcal/mol	+3.9 kcal/mol
GS D	B3LYP/ 6-31G	+4.4 kcal/mol	+4.0 kcal/mol
	ωB97X-D/ 6-311G(d,p)	+5.0 kcal/mol	+5.2 kcal/mol
GS E	B3LYP/ 6-31G	+16.1 kcal/mol	+13.1 kcal/mol
	ωB97X-D/ 6-311G(d,p)	+9.0 kcal/mol	+9.6 kcal/mol
TS A	ωB97X-D/ 6-311G(d,p)	+31.4 kcal/mol [3]	+38.5 kcal/mol [3]
TS B	ωB97X-D/ 6-311G(d,p)	+41.1 kcal/mol [3]	+44.2 kcal/mol [3]

[1] Ar = 2,4-dinitrophenyl. [2] Thermally corrected at 413.15 K. [3] Accounting for alcohol and water.

Table 2. Library of 2-HOBPOs examined computationally, with energetic spans reported as $\Delta G^{\ddagger}$ vs. **GS B**, and accounting for liberated water and 1-phenylpropan-2-ol.

Structure	R_2	Compound	$\Delta G^{\ddagger}$ (TS A) (kcal/mol)	Imaginary Mode (cm^{-1})	$\Delta G^{\ddagger}$ (TS B) (kcal/mol)	Imaginary Mode (cm^{-1})
	Ph	**1a**	38.5	−393	44.2	−359
	Me	**2a* [1]**	36.6	−386	44.1	−329
	Ph	**1b**	36.9	−388	44.5	−349
	Me	**2b* [1]**	37.4	−386	44.4	−331
	Ph	**1c**	35.8	−381	43.5	−355
	Me	**2c* [1]**	36.0	−388	43.3	−323
	Ph	**1d**	35.6	−369	43.6	−315
	Me	**2d* [1]**	35.7	−382	47.0	−301

[1] Aliphatic substituents on phosphorus were modeled as the truncated methyl groups to reduce computation time.
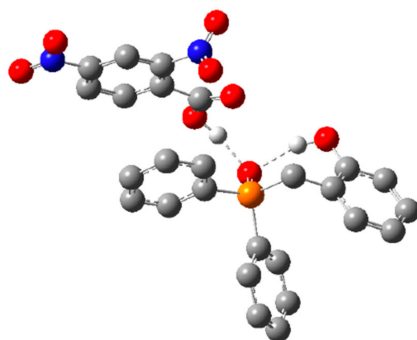
Figure 6. Optimized ground state structure **GS B** for **1a** and DNBA. Hydrogen atoms not involved in hydrogen bonding have been omitted for clarity. Hydrogen atoms shown in white, carbon atoms shown in gray, nitrogen atoms shown in blue, oxygen atoms shown in red, and phosphorus atoms shown in orange.

While the relative stabilities of all of the intermediates and transition states changed by up to 5 kcal/mol across the set of analogs investigated, in all cases, the global minimum and global maximum energies were associated with the same generic structures, corresponding to modified versions of **GS B** and **TS A**. So, it appears that this set of 2-HOBPO catalysts would all act through similar mechanisms, with the energetic spans defined by the relative stabilities of **GS B** and **TS A** (listed in Table 2).

There is also some variation in the imaginary vibrational modes associated with each transition state. The **TS A** vibrations for **1a**–**1d** range from –393 cm^{-1} to –369 cm^{-1}, while the **TS A** vibrations for **2a***–**2d*** range from –388 cm^{-1} to –382 cm^{-1}. In both cases, the nitro-substituted analogs **1d** and **2d*** had the smallest frequency. The **TS B** vibrations for **1a**–**1d** range from –359 cm^{-1} to –315 cm^{-1}, while the **TS B** vibrations for **2a***–**2d*** range from –331 cm^{-1} to –301 cm^{-1}. Again, with the nitro-substituted analogs, **1d** and **2d*** have the smallest frequency. The difference between the *P*-phenylated **1** series and the *P*-methylated **2*** series was found to be significantly larger for **TS B** than for **TS A**.

2.2. Synthesis of 2-HOBPO Catalyst Candidates

In contrast to the multi-step synthesis of **1a** reported previously [1], the 2-HOBPOs examined in this study (Table 3) were each prepared by a single-step ARC reaction [17–19] of a 2° phosphine (Ph_2PH or Et_2PH) and a salicylaldehyde. Due to the gaseous state and extreme pyrophoric and toxic hazards of Me_2PH [21], synthesis of 2-HOBPOs bearing dimethylphosphinoyl substituents (**2x***) was not attempted by ARC.

Table 3. Library of 2-HOBPOs synthesized and examined.

Structure	R$_2$	Compound	Yield [1]	^{31}P (δ) [2]
	Ph	**1a**	89%	37.9
	Et	**2a**	67%	58.5
	Ph	**1b**	88%	38.1
	Et	**2b**	18% [3]	58.0
	Ph	**1c**	74%	38.0
	Et	**2c**	76%	58.6
	Ph	**1d**	77%	36.4
	Et	**2d**	92%	61.6
	Ph	**1e**	39%	38.6
	Et	**2e**	37% [3]	58.7

[1] Un-optimized yields. [2] In 162 MHz, in $CDCl_3$. [3] Poorly suited for crystallization.

2.2.1. Small-Scale Syntheses (<20 mmol)

In general, when performed on a small scale, these reactions produce the corresponding 2-HOBPO with high yield and purity. In the crude mixtures, the only impurities found were traces of unreacted aldehyde, the 2° phosphine oxide derived from partial oxidation of the starting phosphine, the phosphinic acid derived from the complete oxidation of the starting phosphine, or an α-hydroxy-2-HOBPO, which is either produced when the 1,2-addition intermediate is oxidized before the rearrangement can occur (addition-oxidation) or from the 1,2-addition of secondary phosphine oxide to the aldehyde (oxidation-addition) (Figure 7).

The reaction efficiency was sufficiently high, and the workup by aqueous/organic extraction followed by single recrystallization afforded 2-HOBPO in reasonable yields for most products (65–92%, except for **2b**, **1e**, and **2e**) and excellent purity. While it is possible to achieve higher yields through the collection of additional crops of crystals or by flash chromatography of the crude product, for the purposes of this study, it was deemed not to be worth the additional time, labor, and solvent.

2.2.2. Large-Scale (30–50 mmol) Synthesis

Finally, to demonstrate the reproducibility, scalability, and sustainability of this preparative methodology, **1a** was synthesized twice on a >30-mmol scale from equimolar amounts

of diphenylphosphine and salicylaldehyde in TFA. After the completion of the reactions, roughly one-third of the TFA could be recovered by distillation for reuse. The distilled TFA was found to have no phosphorus-containing impurities and only traces of salicylaldehyde. The recycled TFA was used again for an additional synthesis of **1a** (Table S1, reaction #4), which proceeded no differently than when using TFA straight from the bottle. By recovering TFA by distillation, and using recrystallization as the only means of purification, roughly decagram quantities of the product could be prepared with an E-factor of 10.8 (ca. 108 g of waste produced per 10 g of **1a**).
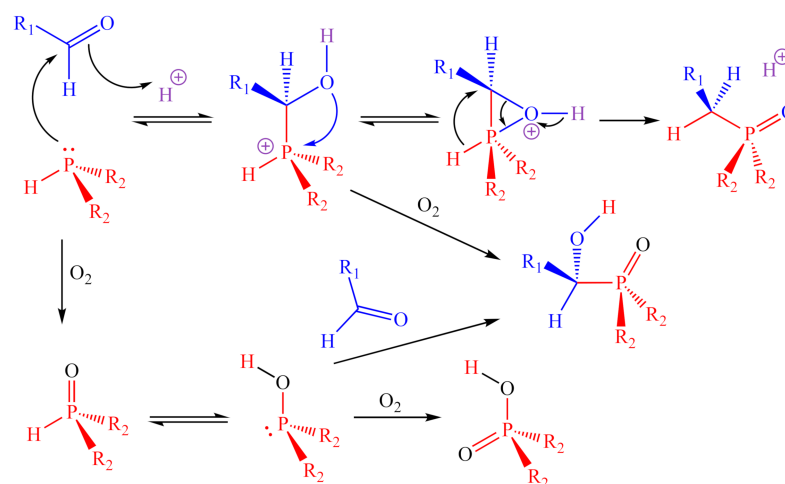
Figure 7. Proposed mechanisms for the ARC synthesis, as well as for the observed side products.

2.3. Kinetics Studies

2.3.1. Rate Law of 2-Octanol and 2,4-DNBA Catalyzed by **1a**

The logarithmic form of the rate law takes the form of Equation (1):

$$\log(\text{rate}) = \log(k) + a \log([2 - \text{octanol}]) + b \log([2,4 - \text{DNBA}]) + c \log([2 - \text{HOBPO}]) \tag{1}$$

To determine coefficient a, reactions were set up with concentrations of 2-octanol over a range of 0.03–0.10 molal (corresponding to ca. 0.026–0.086 molar at 300 K or 0.023–0.075 molar at 413 K, due to the thermal expansion of the solvent [22]), with fixed concentrations of 2,4-DNBA and **1a**. Coefficient b was determined in the same way, but by varying concentrations of 2,4-DNBA over a range of 0.03–0.10 molal. Finally, coefficient c was determined by examining reactions set up with concentrations of **1a** over a range of 0.001–0.085 molal (1.3–85 mol% with respect to 2,4-DNBA), with fixed concentrations of 2-octanol and 2,4-DNBA.

The rate law was determined to have values of k = 6.47, a = 0.79, b = 0.70, and c = 0.49. The fact coefficients a, b, and c are non-integral suggests the possibility of multiple competing mechanisms or, more likely, a single active mechanism that is of the first order in each component, but as concentrations increase, each component can increasingly participate in the equilibration with inactive, off-cycle species.

2.3.2. TOF as a Function of 2-HOBPO Loading

Each of the 10 2-HOBPO catalyst candidates was examined over a range of 0.001–0.01 molal (1.3–13.0 mol% with respect to 2,4-DNBA), similar to the determination of coefficient c of the rate law corresponding to **1a**.

All catalysts examined appeared to demonstrate the same auto-inhibition effect observed with **1a**. Interestingly, there appear to be significant differences in both the inherent activity of the catalyst and in their propensity to inhibit reactivity at higher concentrations. A comparison of log(TOF)/log([2-HOBPO]) relationships (Figure 8a) demonstrates the

interplay between these two factors, showing that the relative ordering of activity is highly concentration dependent.

(a)　　　　　　　　　　　　　　　　　　　(b)
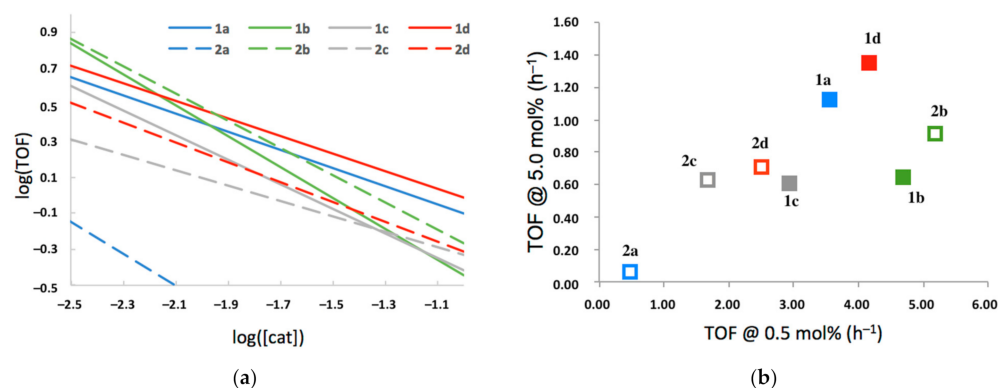
Figure 8. (**a**) Linear fits of log(TOF) as a function of log([2-HOBPO]) at 180 °C in xylenes; (**b**) a comparison of initial-rate TOF of each 2-HOBPO at 0.5 mol% loading and at 5.0 mol% loading.

By plotting each catalyst with coordinates based on their modeled TOF at a low loading of 0.5 mol% and at a high loading of 5.0 mol% (Figure 8b), it can be seen that the catalyst with the highest observed TOF in this study (**2b**) is not the same as the catalyst with the highest observed rate (**1d**). Selected data shown graphically in Figure 7 is shown in tabular format in Table 4.

Table 4. Comparison of initial-rate turnover frequencies for the 2-HOBPOs examined in xylenes at 180 °C, both as a function of catalyst loading and at high loading.

Catalyst	TOF @ 0.5 mol%	TOF @ 5 mol%	log(TOF)/log([2-HOBPO])
1a	$3.56\,h^{-1}$	$1.12\,h^{-1}$	-0.50
2a	$0.47\,h^{-1}$	$0.06\,h^{-1}$	-0.88
1b	$4.66\,h^{-1}$	$0.65\,h^{-1}$	-0.86
2b	$5.17\,h^{-1}$	$0.91\,h^{-1}$	-0.75
1c	$2.94\,h^{-1}$	$0.61\,h^{-1}$	-0.68
2c	$1.67\,h^{-1}$	$0.62\,h^{-1}$	-0.43
1d	$4.16\,h^{-1}$	$1.36\,h^{-1}$	-0.49
2d	$2.52\,h^{-1}$	$0.71\,h^{-1}$	-0.55
1e [1]	N/A	N/A	N/A
2e [1]	N/A	N/A	N/A

[1] 2-HOBPO **1e** and **2e** were indistinguishable from the background and interpreted as inactive.

3. Discussion

3.1. Interpretation of Rate Law Data

The observed rate law appears to be in agreement with the mechanism proposed by Houk and co-workers (in which the turnover-limiting transition state contains one molecule each of catalyst, alcohol, and pronucleophile), while being inconsistent with that proposed by Denton and co-workers (in which the turnover-limiting transition state involves only the catalyst and pronucleophile).

One could reasonably expect the mechanism in which the highest energy transition state is that of the nucleophilic substitution of the nucleophile and activated alcohol to be of the first order in all three components of the reaction (catalyst, alcohol, and pronucleophile): The concentration of the activated alcohol can be viewed as a rapidly maintained equilibrium concentration defined by Equation (2), which can be restated as Equation (3). Then the rate of the substitution could be expressed as Equation (4) or (5):

$$\text{Keq} = [\text{activated alcohol}] / [\text{alcohol}]\,[\text{catalyst}] \tag{2}$$

$$[\text{activated alcohol}] = \text{Keq}\,[\text{alcohol}]\,[\text{catalyst}] \tag{3}$$

$$\text{rate} \ = \ k \, [\text{Nu--}] \, [\text{activated alcohol}] \tag{4}$$

$$\text{rate} \ = \ k \, [\text{Nu--}] \, \text{Keq} \, [\text{alcohol}] \, [\text{catalyst}] \tag{5}$$

When 2-HOBPO **1a** is used as the catalyst in xylenes in a 180 °C heating block, the reaction is nearly first order with respect to both the pronucleophile and alcohol. At this time, it is not entirely clear why the order deviates from whole numbers, but it is clear that it does. Possible explanations include multiple competing productive mechanisms, inhibition by interception of electrophilic intermediates, H-bonding interference, etc.

Because of the high selectivity for the inversion of the alcohol center observed for **1a**-facilitated reactions, the possibility of multiple substitutions at that center can be ruled out with high certainty. For example, one could imagine that the activated alcohol could be intercepted by another equivalent of the nucleophilic phosphine oxide catalyst (Figure 9a), which could displace the phosphine oxide originally bound to the activated alcohol. Because this elementary step would result in the inversion of the stereochemistry of the alcohol at that center, any significant amount of equilibration of this type would result in epimerization, which was not observed by Denton and co-workers [1]. Instead, it could be that hydrogen-bonding interactions could be responsible, either for deactivating the catalyst (Figure 9b), increasing the apparent energetic span of the catalytic cycle either by adding a more stable ground state or increasing the number of energetically similar ground states of possible or for deactivating the nucleophile, effectively increasing the activation barrier for the nucleophilic substitution (Figure 9c–e). Additional experimental and computational studies will be required to identify which of these mechanisms (if any) is responsible.

3.2. Comparison of Computational and Experimental Findings

The calculated energetic spans of gas-phase reactions presented in Section 2 are largely in agreement with the observed TOF values at low catalyst concentrations, in that both computed and experimentally derived energetic spans are within 3 kcal/mol of each other, representing an absolute error of ≤10%. However, when comparing these computed and experimentally determined values (Figure 10), it appears that the 2-HOBPO catalysts fall into two classes: The catalysts with the highest turnover frequencies at low loading (**1a**, **1b**, **2b**, and possibly **1d**), for which the computed and experimental values are in poor agreement, and the remainder of the 2-HOBPOs studied (**1c**, **2a**, **2c**, **2d**, and possibly **1d**), which appear to be in excellent agreement with computed values.

One potential explanation of these findings is that the two groups of catalysts operate by different mechanisms—with the less-active catalysts following the mechanism examined by Houk and co-workers [9] and in this manuscript, while the more-active catalysts follow a different mechanism. If this is the case, it is surprising that such subtle structural differences would result in such dramatic differences.

It is more likely that the computed energies and/or structures of **TS A** or **GS B** for **1a**, **1b**, and **2b*** are inaccurate. It is also possible that **2a** is the only anomalous data point, and that there is poor agreement between computation and experiment. However, it should be emphasized that each of the points in Figure 10 represents the aggregated data from multiple experiments, each with multiple measurements. Future work will require both computation and experimentation on an expanded library of catalyst candidates.

3.3. Mechanistic Insight and SARs

Based on the combined analysis of computational and experimental findings using this small catalyst library, there are a few notable insights into the mechanism, as well as a few salient, preliminary findings regarding the structure–activity relationships of these catalysts. Important takeaways include:

- 2-HOBPO catalysts appear to be auto-inhibitory, with log(TOF) vs. log([2-HOBPO]) having slopes between −0.88 and −0.43.

- Both 2-HOBPOs containing aromatic substituents on the phosphine oxide (**1x**) and those containing aliphatic ones (**2x**) are competent catalysts.
- Only **1e** and **2e**, bearing trifluoromethyl substituents *ortho* to the phenol OH, appear to be completely inactive.
- The rate law appears to be nearly first order in alcohol and pronucleophile, consistent with a rate-determining transition state late in the catalytic cycle.
- There is no obvious relationship between the electron-donating or electron-withdrawing nature of the variable substituents, and the catalytic efficiency of the corresponding catalyst, but both **1b** and **2b**, with methyl substituents para to the phenol, appear to be the most active catalysts at low loadings, indicating significant levels of inherent activity, while at higher concentrations, **1a** and **1d**, with aromatic *p* substituents and electron-neutral or electron-poor phenol, appeared least inhibited at higher concentrations.
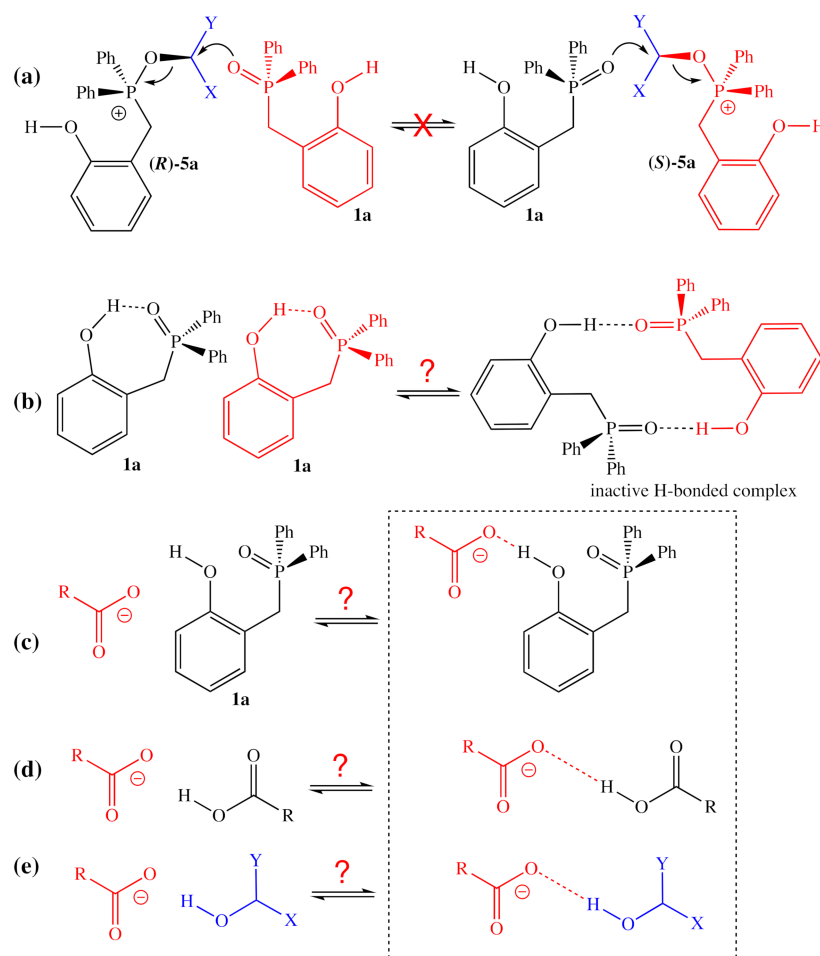
Figure 9. Plausible reactions/interactions which might explain the inhibition observed for increased concentrations of 2-HOBPO, Nu–H, and ROH. (**a**) Implausible exchange of activated alcohol between catalyst molecules; (**b**) possible deactivating hydrogen-bonding between catalyst molecules; (**c**) possible deactivation of nucleophile by excess catalyst; (**d**) possible deactivation of nucleophile by excess pronucleophile; (**e**) possible deactivation of nucleophile by excess alcohol.
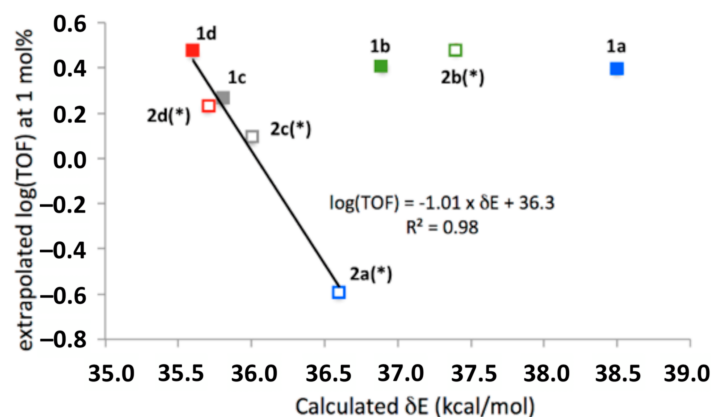
Figure 10. Relationship between low-concentration extrapolation of experimentally determined turnover frequencies and calculated energetic spans of each 2-HOBPO. The * symbol indicates that computational results were obtained for 2-HOBPOs with methyl substituents on phosphorus, and are being compared to experimental results obtained for 2-HOBPOs with ethyl substituents on phosphorus.

4. Materials and Methods

4.1. Materials

Solvents and reagents were used as received, including diphenylphosphine (Alfa Aesar, Tewksbury, MA, USA), diethylphosphine (98%, Sigma Aldrich, Saint Louis, MO, USA), salicylaldehyde (99%, Acros Organics, Geel, Belgium), 5-methylsalicylaldehyde (>98%, TCI America, Portland OR, USA), 5-nitrosalicylaldehyde (>97%, TCI America), 5-methoxysalicylaldehyde (>96%, TCI America), trifluoroacetic acid (99%, Alfa Aesar), deuterochloroform (99.8% D, Cambridge Isotope Laboratories, Tewksbury MA, USA), (±)-2-octanol (97%, Sigma Aldrich), 2,4-dinitrobenzoic acid (98% Alfa Aesar), and xylenes (Alfa Aesar).

4.2. Generic Procedure for ARC Synthesis of 2-HOBPOs

A Teflon-coated stir bar and a 35 mL heavy-walled borosilicate pressure tube (Ace Glass Inc., Vineland, NJ, USA "Tube C", Product #864807) were oven-dried overnight and then allowed to cool to ambient temperature in air. The tube was then charged with the aldehyde, and flushed gently with dry nitrogen gas. Then, while maintaining the gentle nitrogen flush, trifluoroacetic acid was added in a single portion, followed quickly by the phosphine, which was also added swiftly in one portion by syringe. The tube was then sealed with a threaded Teflon cap fitted with a Viton o-ring. The sealed tube was then heated in an 80 °C aluminum-pebble bath behind a blast shield for 8–20 h. The reaction vessel was then removed from the aluminum-pebble bath and allowed to cool to room temperature. Once cool, the reaction tube was opened, and the contents were transferred into a 250 mL separatory funnel that had already been charged with 50 mL of half-saturated sodium bicarbonate (25 mL saturated sodium bicarbonate and 25 mL water). The reaction flask was rinsed with two 25 mL portions of dichloromethane, which were both transferred to the separatory funnel. After agitation, the layers were allowed to separate, and the organic layer was collected. The remaining aqueous phase was extracted with two more portions of dichloromethane (each 50 mL), and the organic phases were all combined, dried over sodium sulfate, and concentrated under vacuum to afford the crude product. All glassware, gloves, and other objects or surfaces that came into contact with phosphines were rinsed immediately in bleach (5% sodium hypochlorite/water) to quench any residual phosphine, followed by water, and finally methanol. A photograph of a 50 mmol reaction setup and distillation setup is available in Figure S1.

4.3. Kinetic Studies

A Radley's Carousel 12 plus parallel reactor was used to simultaneously heat the base of up to 12 reaction tubes to 180 °C while cooling the tops of the tubes to 10 °C with a recirculating chiller (CF302L—A Neocool Circulator, from Yamato Scientific Co. Ltd., Tokyo, Japan). No Dean–Stark apparatus was used for these reactions as the water was driven off by excess heat and condensed along the top of each Radley tube by the recirculating chiller. To determine the reaction order of 2-HOBPO **1a** 14 reactions of various loadings were performed in which 2-octanol (1.30 g, 10.0 mmol) and 1,3,5-trimethoxybenzene (841 mg, 5.0 mmol) were added to a 250 mL Erlenmeyer flask and dissolved in xylenes (100 g) for a stock solution. Each reaction consisted of 2,4-dinitrobenzoic acid (159 mg, 0.75 mmol), 7.5 g of stock solution, and the catalyst loading for **1a** varied over 7 reactions where the catalyst concentration doubled from 0.01 to 0.64 mmol (0.001–0.085 molal, 1.3–85.0 mol%.) The same reaction conditions were repeated a second time.

To determine the substrate effect on the reaction rate with respect to 2,4-dinitrobenzoic acid, loadings were varied over 8 reactions in which 2-octanol (862 mg, 6.62 mmol), 1,3,5-trimethoxybenzene (590 mg, 3.51 mmol), and 2-HOBPO **1a** (64.7 mg, 0.209 mmol) were added to a 250 mL Erlenmeyer flask and dissolved in xylenes (65 g) for a stock solution. Each reaction consisted of 9.2 g of stock solution, and 2,4-dinitrobenzoic acid was varied between reactions (63.3–204.1 mg, 0.29–0.96 mmol).

To determine the substrate effect on the reaction rate with respect to 2-octanol, loadings were varied over 8 reactions in which 1,3,5-trimethoxybenzene (650 mg, 3.86 mmol) and 2-HOBPO **1a** (64.7 mg, 0.146 mmol) were added to a 250 mL Erlenmeyer flask and dissolved in xylenes (79 g) for a stock solution. Each reaction consisted of 7.5 g of the stock solution and 2,4-dinitrobenzoic acid (159 mg, 0.75 mmol), and 2-octanol was varied between reactions (29.4–114 mg, 0.226–0.877 mmol).

To determine reaction rates for novel 2-HOBPO candidates, 2-octanol (2.09 g, 16.0 mmol) and 1,3,5-trimethoxybenzene (891 mg, 5.3 mmol) were added to a 250 mL Erlenmeyer flask and dissolved in xylenes (165 g) for a stock solution. Each reaction consisted of 2,4-dinitrobenzoic acid (159 mg, 0.75 mmol), 7.5 g of stock solution, and loadings were varied over three reactions for each 2-HOBPO (0.01–0.10 mmol, 1.3–13.0 mol%).

Up to 5 aliquots from each reaction were taken hourly after a preliminary four-hour induction period, and the reaction progress was monitored via 400 MHz ^{1}H NMR to derive an instantaneous TOF. The initial reaction progress is nearly indistinguishable from the background within the first three hours of reaction progress, and it is presumed that the initial four-hour period is required to drive off excess water, which would otherwise inhibit the reaction.

5. Conclusions

The ARC reaction is shown to be a synthetically useful single-step method for preparing systematically varied 2-HOBPOs, from aromatic or aliphatic 2° phosphines and salicylaldehydes bearing electron-donating, electron-neutral, and electron-withdrawing substituents. Of a small library of ten 2-HOBPO catalyst candidates, only two of them were found to be catalytically inactive for the reaction of 2-octanol and 2,4-DNBA (those containing a trifluoromethyl group ortho to the OH of the phenol, **1e** and **2e**). Of the remaining eight catalyst candidates, TOF values at 0.5 mol% loading spanned about one order of magnitude, from just under 0.5 h^{-1} (**2a**) to just over 5 h^{-1} (**2b**), while catalyst auto-inhibition also varied markedly. When expressed as log(TOF)/log([2-HOBPO]), all slopes were negative and ranged from −0.88 (**2a**) to −0.43 (**2c**). Compound **1d** was found to be the catalyst capable of providing the highest rate of product formation (at high catalyst loadings), while **2b** was found to operate with the highest TOF (at low loadings).

Future studies will be directed at modeling possible inhibitory interactions and processes computationally, as well as significantly expanding the scope of the combinatorial library of catalyst candidates and examining them both computationally and experimen-

tally. Finally, future studies should examine the activities and selectivities of 2-HOBPO catalysts applied to a wider range of alcoholic and pronucleophilic substrates.

References

1. Beddoe, R.H.; Andrews, K.G.; Magné, V.; Cathbertson, J.D.; Saska, J.; Shannon-Little, A.L.; Shanahan, S.E.; Sneddon, H.F.; Denton, R.M. Redox-neutral organocatalytic Mitsunobu reactions. *Science* **2019**, *365*, 910–914. [CrossRef] [PubMed]
2. Swamy, K.C.K.; Kumar, N.N.B.; Balaraman, E.; Kumar, K.V.P.P. Mitsunobu and related reactions: Advances and applications. *Chem. Rev.* **2009**, *109*, 2551–2651. [CrossRef] [PubMed]
3. Fletcher, S. The Mitsunobu reaction in the 21st century. *Org. Chem. Front.* **2015**, *2*, 739–752. [CrossRef]
4. Tsunoda, T.; Yamamiya, Y.; Itô, S. 1,1′-(azodicarbonyl)dipiperidine-tributylphosphine, a new reagent system for mitsunobu reaction. *Tetrahedron Lett.* **1993**, *34*, 1639–1642. [CrossRef]
5. Jackson, T.; Routledge, A. Synthesis and application of crown ether tagged triarylphosphines. *Tetrahedron* **2003**, *44*, 1305–1307. [CrossRef]
6. Buonomo, J.A.; Aldrich, C.C. Mitsunobu reactions catalytic in phosphine and a fully catalytic system. *Angew. Chem. Int. Ed.* **2015**, *54*, 13041–13044. [CrossRef]
7. But, T.Y.S.; Toy, P.H. Organocatalytic mitsunobu reactions. *J. Am. Chem. Soc.* **2006**, *128*, 9636–9637. [CrossRef]
8. Zhou, L.; Perulli, S.; Mastandrea, M.M.; Llanes, P.; Lai, J.; Pericàs, M.A. Development of a robust immobilized organocatalyst for the redox-neutral mitsunobu reaction. *Green Chem.* **2021**, *23*, 8859–8864. [CrossRef]
9. Zou, Y.; Wong, J.J.; Houk, K.N. Computational exploration of a redox-neutral organocatalytic mitsunobu reaction. *J. Am. Chem. Soc.* **2020**, *142*, 16403–16408. [CrossRef]
10. Chai, J.-D.; Head-Gordon, M. Long-range corrected hybrid density functionals with damped atom-atom dispersion corrections. *Phys. Chem. Chem. Phys.* **2008**, *10*, 6615–6620. [CrossRef]
11. Kozuch, S.; Shaik, S. How to conceptualize catalytic cycles? The energetic span model. *Acc. Chem. Res.* **2011**, *44*, 101–110. [CrossRef] [PubMed]
12. Wittig, G.; Schöllkopf, U. Über Triphenyl-phosphine-methylene als olefinbildende Reagenzian. *Chem. Ber.* **1954**, *87*, 1318–1330. [CrossRef]
13. Golobov, Y.G.; Zhmurova, I.N.; Kasukhin, L.F. Sixty years of Staudinger reaction. *Tetrahedron* **1981**, *37*, 437–472. [CrossRef]
14. Matrosov, E.I.; Tsvetkov, E.N.; Mironova, Z.N.; Malevannaya, R.A.; Kabachnik, M.I. Acid-base properties of phosphine oxides in nitromethane. *Izv. Akad. Nauk. SSSR Seriya Khimicheskaya* **1975**, *6*, 1333–1337. [CrossRef]
15. Gu, X.; Yuan, H.; Jiang, J.; Wu, Y.; Bai, W.-J. Catalytic asymmetric hydrophosphination of *ortho*-quinone methides. *Org. Lett.* **2018**, *20*, 7229–7233. [CrossRef]
16. Tatarinov, D.A.; Kuznetsov, D.M.; Kostin, A.A.; Mironov, V.F. 2-Ethoxy-2,3-dihydro[*d*][1,2]oxaphosphole 2-Oxide in the Synthesis of Dialkyl(diaryl)2-hydroxybenzyl)phosphine Oxides. *Zhurnal Obs. Khimii* **2016**, *86*, 386–390. [CrossRef]

17. Epstein, M.; Buckler, S.A. Reactions of primary and secondary phosphines with aldehydes and ketones. *Tetrahedron* **1962**, *18*, 1231–1242. [CrossRef]
18. Chikkali, S.; Gudat, D. Hydrophosphination of phenolic aldehydes as facile synthetic approach to catechol-functionalized phosphane oxides and phosphanes. *Eur. J. Inorg. Chem.* **2006**, *2006*, 3005–3009. [CrossRef]
19. Bloomfield, A.J.; Qian, J.M.; Herzon, S.B. Single-step synthesis of secondary phosphine oxides. *Organometallics* **2010**, *29*, 4193–4195. [CrossRef]
20. Zhao, Y.; Tishchenko, O.; Truhlar, D.G. How well can density functional methods describe hydrogen bonds to π acceptors? *J. Phys. Chem. B.* **2005**, *109*, 19046–19051. [CrossRef]
21. Trenkle, A.; Vahrenkamp, H.; Svoboda, J.; Brewer, L. 40. Dimethylphosphine. *Inorg. Synth.* **1982**, *21*, 180–181. [CrossRef]
22. Zhou, Y.; Wu, J.; Lemmon, E.W. Thermodynamic properties of *o*-Xylene, *m*-Xylene, *p*-Xylene, and ethylbenzene. *J. Phys. Chem. Ref. Data* **2012**, *41*, 023103. [CrossRef]